

Spatially nonuniform phases in the one-dimensional SU(n) Hubbard model for commensurate fillings

E. Szirmai, Ö. Legeza, and J. Sólyom

Research Institute for Solid State Physics and Optics, P.O. Box 49, H-1525 Budapest, Hungary

(Received 28 August 2007; published 8 January 2008)

The one-dimensional repulsive SU(n) Hubbard model is investigated analytically by bosonization approach and numerically using the density-matrix renormalization-group method for $n=3, 4$, and 5 for commensurate fillings $f=p/q$, where p and q are relatively primes. It is shown that the behavior of the system is drastically different depending on whether $q>n$, $q=n$, or $q<n$. When $q>n$, the umklapp processes are irrelevant and the model is equivalent to an n -component Luttinger liquid with central charge $c=n$. When $q=n$, the charge and spin modes are decoupled, the umklapp processes open a charge gap for finite $U>0$, whereas the spin modes remain gapless and the central charge $c=n-1$. The translational symmetry is not broken in the ground state for any n . On the other hand, when $q<n$, the charge and spin modes are coupled, the umklapp processes open gaps in all excitation branches, and a spatially nonuniform ground state develops. Bond-ordered dimerized, trimerized, or tetramerized phases are found depending on the filling.

DOI: 10.1103/PhysRevB.77.045106

PACS number(s): 71.10.Fd

I. INTRODUCTION

Recently, the SU(n)-symmetric generalization of the standard SU(2) Hubbard model¹ has been intensively studied theoretically.²⁻⁹ Apart from its theoretical interest, this model may mimic strongly correlated electron systems where the orbital degrees of freedom of d and f electrons play an important role and these extra degrees of freedom are taken into account by considering n -component fermions. On the other hand, ultracold gases in optical lattices may also be simulated by such multicomponent models.

The Hamiltonian of the model is usually written in the form

$$\mathcal{H} = -t \sum_{i=1}^N \sum_{\sigma=1}^n (c_{i,\sigma}^\dagger c_{i+1,\sigma} + c_{i+1,\sigma}^\dagger c_{i,\sigma}) + \frac{U}{2} \sum_{i=1}^N \sum_{\substack{\sigma,\sigma'=1 \\ \sigma \neq \sigma'}}^n n_{i,\sigma} n_{i,\sigma'}, \quad (1)$$

where N is the number of sites in the chain. The operator $c_{i,\sigma}^\dagger$ ($c_{i,\sigma}$) creates (annihilates) an electron at site i with spin σ , where the spin index is allowed to take n different values. $n_{i,\sigma}$ is the particle-number operator, t is the hopping integral between nearest-neighbor sites, and U is the strength of the on-site Coulomb repulsion. In what follows, t will be taken as the unit of energy.

The model behaves as an n -component Tomonaga-Luttinger liquid at generic fillings. Other types of behavior may appear at commensurate fillings due to umklapp processes. The possible phases, their nature, and the critical coupling where they appear have been studied in detail for two special commensurate fillings of the band, namely, for half filling and $1/n$ filling.²⁻⁹ It is well established by now that the ground state is a fully gapped bond-ordered dimerized state in the half-filled case for any $n>2$. Contrary to this, the ground state remains translationally invariant in the $1/n$ -filled case, and only the charge mode acquires a gap for $U>U_c$. While Assaraf *et al.*³ argued that U_c is finite, our recent numerical work⁹ has suggested a much less, perhaps

$U_c=0$ critical value above which multiparticle umklapp processes become relevant.

It is worth mentioning that the SU(n) Hubbard model has a rich phase diagram in the attractive case, too.^{10,11} The one-third-filled SU(3) model has two distinct phases in the high-dimensional limit. In one of them, the fermions form trions, while in the other phase, a color superfluid state emerges. The existence of these phases is not yet settled in one dimension.

In the present paper, the role of multiparticle umklapp processes will be further analyzed for general commensurate fillings $f=p/q$, where p and q are relatively primes. We try to establish under what conditions the umklapp processes can generate gaps in the charge or spin sectors, and when and how the translational symmetry is broken. To this end, partly analytic, partly numerical procedures will be applied. We will generalize the method used in Ref. 2 to the one-third-filled SU(n) model to show analytically that the ground state cannot be spatially uniform. It is trimerized at least in the large- n limit. The numerical work will show that, in fact, this trimerized state with gapped excitations exists for $n>3$ already.

In the numerical part, the length dependence of the entropy of finite blocks of a long chain is studied. Recently, it has been shown that quantum phase transitions can be conveniently studied by calculating some measure of entanglement.¹²⁻²⁰ This can either be a local quantity, e.g., the concurrence,²¹ a global quantity, e.g., the fidelity,²² or the entropy of a block of several sites.²³ As has been demonstrated recently,²⁴ the oscillatory behavior of the block entropy can reveal the position of soft modes in the excitation spectrum of critical systems or the spatial inhomogeneity of gapped models. This will allow us to demonstrate that at commensurate fillings $f=p/q$, the type of ground state of the one-dimensional SU(n) models depends on whether $q=n$, $q<n$, or $q>n$.

The paper is organized as follows. The oscillatory behavior of the block entropy, the corresponding peaks in its Fourier spectrum, and their relationship to the known properties

of the half-filled and $1/n$ -filled models are recalled in Sec. II, where some results necessitating further studies are also given. An analytical investigation of the role of umklapp processes at commensurate fillings is presented in Sec. III and the possibility of spatial inhomogeneity of the ground state is discussed. The numerical results for various fillings are presented in Sec. IV. Finally, our findings and conclusions are summarized in Sec. V.

II. OSCILLATORY LENGTH DEPENDENCE OF THE BLOCK ENTROPY

If a finite block of length l of a long chain of N sites is considered, it is in a mixed state, even if the long chain is in its ground state. The mixed state can be described by a density matrix $\rho_N(l)$ and the corresponding von Neumann entropy is

$$s_N(l) = -\text{Tr}[\rho_N(l)\ln\rho_N(l)]. \quad (2)$$

It is well known^{23,25} that this entropy as a function of the block size grows logarithmically if the system is critical and the spectrum is gapless. In addition, the central charge c can be derived^{26,27} from the initial slope of the length dependence of $s_N(l)$,

$$s_N(l) = \frac{c}{6} \ln\left[\frac{2N}{\pi} \sin\left(\frac{\pi l}{N}\right)\right] + g, \quad (3)$$

where g is a shift due to the open boundary. It contains a constant term which depends on the ground-state degeneracy and an alternating term decaying with a power of the distance from the boundary.^{28,29} On the other hand, for noncritical, gapped models, $s_N(l)$ saturates to a finite value when l is far from the boundaries.

Recently, it has been pointed out by some of us²⁴ that a wider variety of behavior may be found for the length dependence of the block entropy. Namely, we have shown that in some cases, oscillations may appear in $s_N(l)$. This can be best analyzed by considering the Fourier transform

$$\tilde{s}(k) = \frac{1}{N} \sum_{l=0}^N e^{-ikl} s_N(l), \quad (4)$$

for discrete wave numbers, where $k=2\pi j/N$ lying in the range $(-\pi, \pi)$. Since $s_N(l)=s_N(N-l)$, $\tilde{s}(k)$ is real. It has a large peak at $k=0$ and all other Fourier components are negative. Peaks in $|\tilde{s}(k)|$ carry information about the position of soft modes or the spatial inhomogeneity of the ground state. More precisely, if the amplitude of a peak at a nonzero wave number k^* remains finite in the thermodynamic limit, this indicates a periodic spatial modulation of the ground state with wavelength $\lambda=2\pi/k^*$. On the other hand, if a marked peak appears in $|\tilde{s}(k)|$ but its amplitude vanishes as $N\rightarrow\infty$, this allows us to identify the wave vector of soft modes in critical models.

In a recent work,⁹ we have shown that such oscillations appear in $s_N(l)$ for the $SU(n)$ Hubbard model as well. The periodicity depends on both n and the band filling $f=p/q$. This is shown for the $n=3$ and $n=4$ models for the $1/n$ -

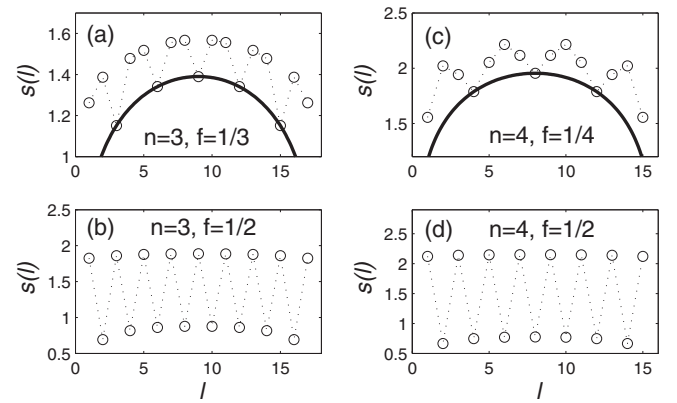


FIG. 1. Block entropy $s_N(l)$ of finite chains with $N=18$ and $N=16$ sites, respectively, for $n=3$ and 4 at fillings $f=1/n$ and $f=1/2$ for $U=10$. The solid line is our fit using Eq. (3).

filled and half-filled cases in Fig. 1 for a large value of U ($U=10$).

In the $1/n$ -filled cases, $s_N(l)$ increases logarithmically with the block length (and then goes down as l approaches N). When every third or fourth values are taken, depending on the periodicity, these selected values can be fitted to (3), as shown by the solid lines in panels (a) and (c). This indicates a gapless behavior and gives $c=n-1$. This is in agreement with the theoretical expectation since the charge mode becomes gapped due to multiparticle umklapp processes and only the $n-1$ spin modes are gapless. A distinct behavior is found in half-filled systems, as seen in panels (b) and (d). The quantity $s_N(l)$ oscillates with period 2, and if only every second point is taken, it seems to saturate beyond some block length, before decreasing again, indicating that the corresponding models are fully gapped.

The finite-size dependence of the peaks of $|\tilde{s}(k)|$ appearing at $k^*=2k_F=2\pi f$ characterizing the oscillation is shown in Fig. 2. It is seen that in the $1/n$ -filled case, the Fourier components at $k^*=2\pi/n$ vanish in the thermodynamic limit, while a finite value is obtained at $k^*=\pi$ for half-filled mod-

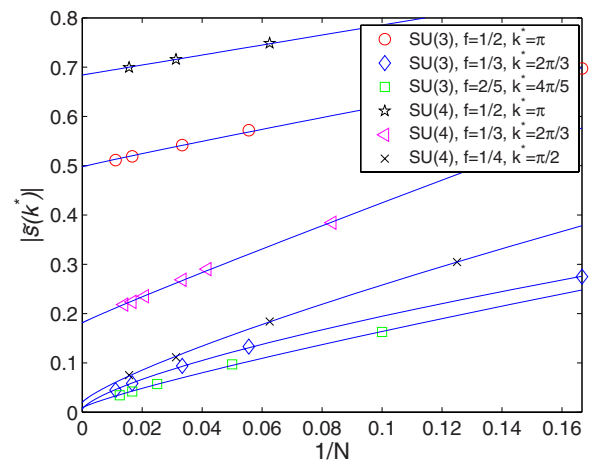


FIG. 2. (Color online) Finite-size dependence of $|\tilde{s}(k^*)|$ for various n and fillings for $U=10$. The solid line is the finite-size-scaling fit.

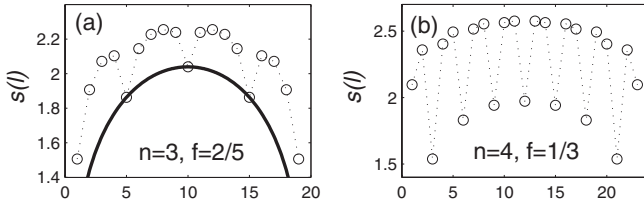


FIG. 3. Same as Fig. 1 but for (a) $n=3$, $f=2/5$, $N=20$ and (b) $n=4$, $f=1/3$, $N=24$.

els. This corroborates our finding that the $1/n$ -filled $SU(n)$ models are critical with a spatially uniform ground state, while a gapped bond-ordered dimerized phase appears at half filling.

We have done similar calculations for more general commensurate fillings of the band. Figure 3 shows the results obtained for $n=3$, $f=2/5$ as well as for $n=4$, $f=1/3$. When every fifth points are taken for the $f=2/5$ filled $SU(3)$ model, they can be fitted to (3), yielding $c=3$ for the central charge. This indicates that all modes, including the charge mode, are gapless.

Such a fit does not work for the one-third-filled $SU(4)$ model. To better see the difference, $|\bar{s}(k)|$ is considered again. The amplitude of the Fourier component at $k^*=4\pi/5$, also displayed in Fig. 2 for the $n=3$ model, vanishes in the $N \rightarrow \infty$ limit. On the other hand, $|\bar{s}(k)|$ remains finite at $k^*=2\pi/3$ in the one-third-filled $n=4$ model.

When the same calculations are repeated for the $n=5$ model at $f=1/2, 1/3, 1/4$, and $1/5$, peaks appear in $|\bar{s}(k)|$ at $k^*=\pi, 2\pi/3, \pi/2$, and $2\pi/5$, respectively. As is seen in Fig. 4, the amplitude of the peaks remains finite even when $N \rightarrow \infty$ in the first three cases, while it vanishes in the last case.

These results indicate that the role of umklapp processes depends on the relationship between the number of components n and the relative primes p and q characterizing the commensurate filling. In what follows, this problem will be studied first analytically in a bosonization approach and large- n expansion technique, and then numerically using the density-matrix renormalization-group (DMRG) method.

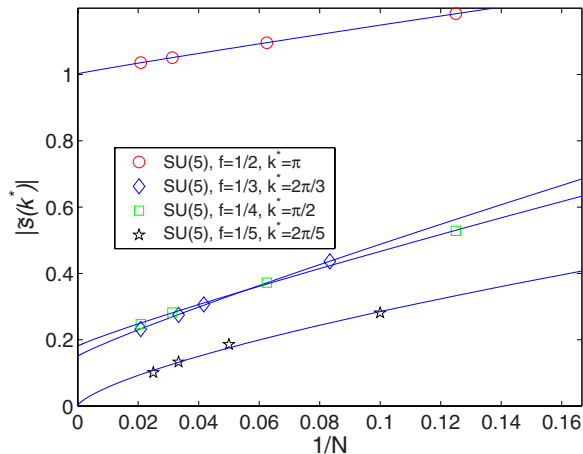


FIG. 4. (Color online) Same as Fig. 2 but for $n=5$. The solid line is the finite-size-scaling fit.

III. ANALYTICAL CONSIDERATIONS

A. Role of umklapp processes: A bosonization approach

Following the usual procedure, we write the Hamiltonian [Eq. (1)] in momentum space and linearize the free-particle spectrum around the two Fermi points ($\pm k_F$). The underlying assumption is that the low-lying excitations determine the physics of the system. Depending on whether the momentum of the fermions is close to $+k_F$ or $-k_F$, one can distinguish left- and right-moving particles, and the interaction processes can also be classified on the basis of whether the incoming and scattered particles are right or left movers and the momentum transfer is small (forward scattering) or large, of the order of $2k_F$ (backward scattering). In a generic model, the strength of the various scattering processes may be different. For the sake of simplicity, we neglect chiral processes in which both particles move in the same direction before and after the interaction since they lead to the renormalization of the Fermi velocity only.

One can recognize that at generic fillings, where umklapp processes do not play a role, the forward- and backward-scattering processes can be interpreted as current-current interactions and their contribution to the Hamiltonian density can be conveniently rewritten using Dirac fermions³⁰ in the following short form (automatic summation for the repeated indices is understood):

$$H_{\text{int}}(x) = \frac{1}{2} g_{\sigma_1 \sigma_2 \sigma_3 \sigma_4} \bar{\psi}_{\sigma_1}(x) \gamma_{\mu} \psi_{\sigma_2}(x) \bar{\psi}_{\sigma_3}(x) \gamma_{\mu} \psi_{\sigma_4}(x). \quad (5)$$

Here, σ_i denote the spin indices that can take the values $1, \dots, n$, γ_{μ} with $\mu=1, 2$ are the Dirac matrices, in our case the standard Pauli matrices (σ_x, σ_y), and $\bar{\psi}(x) = \psi^{\dagger}(x) \gamma_1$. While the Hubbard model contains a single interaction parameter U , the couplings $g_{\sigma_1 \sigma_2 \sigma_3 \sigma_4}$ may be different for physically different processes in more realistic models. In the renormalization-group treatment, we will assume this to be the case. It is assumed, however, that the spin of the fermions does not change in the scattering process and the couplings are symmetric under the exchange $(\sigma_1, \sigma_2) \leftrightarrow (\sigma_3, \sigma_4)$. If the fermion field $\psi_{\sigma}(x)$ is decomposed into left- and right-moving components according to

$$\psi_{\sigma}(x) = \begin{pmatrix} R_{\sigma}(x) \\ L_{\sigma}(x) \end{pmatrix}, \quad \bar{\psi}_{\sigma}(x) = (L_{\sigma}^{\dagger}(x), R_{\sigma}^{\dagger}(x)), \quad (6)$$

the usual backward- and forward-scattering processes are, in fact, recovered. In the standard g -ology³¹ notation, $g_{\sigma\sigma'\sigma''\sigma}$ is denoted by $-g_1$, and $g_{\sigma\sigma'\sigma''\sigma'}$ by g_2 .

The well-known RG equations, the β function, can be written for these scattering processes in a short form,³⁰

$$\begin{aligned} \frac{\partial \ln g_{\sigma_1 \sigma_2 \sigma_3 \sigma_4}}{\partial \ln \Lambda' / \Lambda} &\equiv \beta_{\sigma_1 \sigma_2 \sigma_3 \sigma_4} = g_{\sigma_1 \sigma_i \sigma_3 \sigma_j} g_{\sigma_i \sigma_2 \sigma_j \sigma_4} \\ &\quad - g_{\sigma_1 \sigma_i \sigma_j \sigma_4} g_{\sigma_i \sigma_2 \sigma_3 \sigma_j}, \end{aligned} \quad (7)$$

where Λ is the cutoff parameter. These RG equations have been analyzed earlier^{2,7} and it was found that the backward-scattering processes scale out at generic fillings in the $SU(n)$ Hubbard model and, for this reason, this model is equivalent

to an n -component Luttinger liquid in this case. The Hamiltonian can be diagonalized⁸ and the excitation spectrum can be determined exactly in bosonic phase-field representation.³² There is one symmetric combination of the phase fields with different spin indices, this is the so-called charge mode,

$$\phi_c(x) = \frac{1}{\sqrt{n}} \sum_{\sigma=1}^n \phi_{\sigma}(x), \quad (8)$$

while the $n-1$ antisymmetric combinations give the spin modes,

$$\phi_{ms}(x) = \frac{1}{\sqrt{m(m+1)}} \left[\sum_{\sigma=1}^m \phi_{\sigma}(x) - m\phi_{m+1}(x) \right], \quad (9)$$

with $n=1, \dots, n-1$.

Similarly to the spin-charge separation in the two-component Luttinger model, one finds complete mode separation. The Hamiltonian density is the sum of the contributions of the individual modes,

$$H(x) = \sum_j H_j(x), \quad (10)$$

where $j=c, 1s, 2s, \dots, (n-1)s$. Each term has the usual bosonic form

$$H_j(x) = \frac{\hbar u_j}{2} \left\{ \pi K_j [\Pi_j(x)]^2 + \frac{1}{\pi K_j} [\partial_x \phi_j(x)]^2 \right\}, \quad (11)$$

where $\Pi_j(x)$ is the momentum canonically conjugated to $\phi_j(x)$. The renormalized velocities and the Luttinger parameters can be given in terms of the new couplings $g_{2;j}$ appearing after diagonalization⁸ in the spin indices

$$u_j = v_F \sqrt{1 - g_{2;j}^2}, \quad (12a)$$

$$K_j = \sqrt{\frac{1 - g_{2;j}}{1 + g_{2;j}}}. \quad (12b)$$

In a finite system, where the momentum is quantized in units of $2\pi/L$, the excitation spectrum of the Luttinger model can be written as³³

$$E = \sum_j \hbar u_j \frac{2\pi}{L} (n_+^j + n_-^j + \Delta_+^j + \Delta_-^j), \quad (13)$$

where n_{\pm}^j are integers describing the bosonic excitations and

$$\Delta_{\pm}^j = \frac{1}{16} \left(\sqrt{K_j} J_j \pm \frac{1}{\sqrt{K_j}} \delta N_j \right)^2, \quad (14)$$

where δN_j is the change in the number of particles in the j th channel, and similarly J_j describes the current in the j th channel created by adding particles to or removing them from the branches of the dispersion relation.

The total momentum is given by

$$P = \hbar k_F J_c + \sum_j \hbar \frac{2\pi}{L} (n_+^j - n_-^j + \Delta_+^j - \Delta_-^j). \quad (15)$$

Thus, soft modes appear not only at zero momentum but at integer multiples of $2k_F$, too, since the charge current J_c is an even number if the total charge is conserved. Since

$$2k_F = \frac{N_c^0}{n} \frac{2\pi}{L}, \quad (16)$$

where N_c^0 is the number of particles in the system, and the filling of the band is $f = N_c^0/nN$, the position of these soft modes depends on the filling only, $2k_F = 2\pi f$.

We know that the usual umklapp processes, scattering of two right movers into left-moving states or vice versa, which were neglected so far, are relevant in a half-filled system for any n .^{2,7} Multiparticle umklapp processes may become relevant at other commensurate fillings. To see what kind of processes are allowed, we have to take into account that the total quasimomentum transferred in an umklapp process has to be an integer multiple of 2π . If the band is $f=p/q$ filled and consequently $k_F = p\pi/q$, q particles have to be scattered from one Fermi point to the opposite one to satisfy this condition. The term in the renormalized Hamiltonian that describes these processes is

$$H_U = g_3 \sum_{\{k_j\}, \{k'_j\}} \sum_{\{\sigma_j\}} c_{k_1, \sigma_1}^\dagger c_{k_2, \sigma_2}^\dagger \cdots c_{k_q, \sigma_q}^\dagger c_{k'_q, \sigma_q} c_{k'_q, \sigma_q} \cdots c_{k_2, \sigma_2} c_{k_1, \sigma_1}, \quad (17)$$

where

$$k_1 + k_2 + \cdots + k_q = k'_1 + k'_2 + \cdots + k'_q \pm 2\pi. \quad (18)$$

Due to Pauli's exclusion principle, the spin indices $\sigma_1, \sigma_2, \dots, \sigma_q$ have to be different. Since there are n different types of fermion in the $SU(n)$ model, and the Hubbard interaction is local, only such umklapp processes are allowed in which the number of scattered particles is less than or equal to n . Thus, q -particle umklapp processes are forbidden in our model when $q > n$. Figure 5 shows allowed umklapp processes for the $SU(3)$ model.

The role of multiparticle umklapp processes in the conductivity of the $SU(2)$ Hubbard model has been studied in Ref. 34. A different aspect, whether the charge and spin modes are coupled or not by the possible multiparticle umklapp processes, has been considered for the $SU(n)$ model.⁹ The q -particle umklapp processes of Eq. (17) are described in the bosonic phase-field representation by

$$H_U = g_3 \int dx \sum_{\{\sigma_j\}'} \cos\{2[\phi_{\sigma_1}(x) + \cdots + \phi_{\sigma_q}(x)]\}. \quad (19)$$

The phase fields appearing here are the phases of the bosonic representation of the particles participating in the scattering process, and $\{\sigma_j\}'$ indicates that all spin indices have to be different.

This Hamiltonian can be expressed in terms of the phase fields corresponding to the charge and spin modes, making

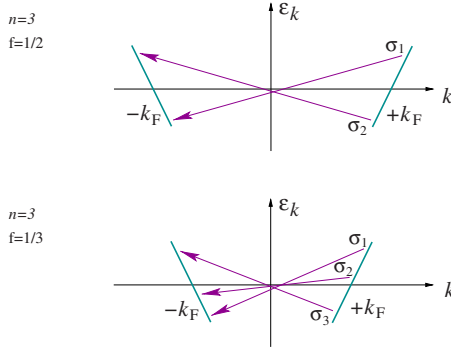


FIG. 5. (Color online) Umklapp processes in the SU(3) symmetric Hubbard model. (a) Any two of the three types of fermion can be scattered in the half-filled case. (b) Fermions with the three possible spin orientations participate in the scattering process in the one-third-filled case.

use of the inverse of Eqs. (8) and (9). It is clear that if $q=n$, only the symmetric combination of the phase fields that is the charge mode defined in Eq. (8) appears in Eq. (19). This means that in this case, the q -particle umklapp processes couple to the charge mode only. The Hamiltonian density of the charge mode is identical to that of the well-known sine-Gordon model which has a fully gapped excitation spectrum. Thus, the charge mode becomes gapped for finite U . The $n-1$ spin modes are not influenced by the umklapp processes in the $1/n$ -filled case. They remain gapless and the central charge is $c=n-1$.

When $q < n$, the sum of the q phase fields corresponding to the q particles required for umklapp processes will contain various combinations of the n boson fields, leading to a mixing (coupling) of the charge and spin modes, thus opening gaps in all modes. The model becomes noncritical for $U > U_c$.

When, on the other hand, $q > n$, umklapp processes are forbidden by Pauli's exclusion principle when the interaction is local. The charge and spin modes remain gapless; thus, $c=n$ for $U > 0$. The expected behavior for different cases is summarized in Table I.

B. Spatial inhomogeneity in the large- n limit of the SU(n) Hubbard-Heisenberg model at one-third filling

We have seen that the spectrum is fully gapped when $q < n$. The question naturally arises whether the opening of a gap at multiples of $k^* = 2k_F$ is related to a breaking of the translational symmetry, an instability against the formation

TABLE I. Central charge c and the type of phase characterized by the number of soft modes in the charge and spin sectors ($C \times S_y$) for the p/q -filled SU(n) Hubbard model.

	n	c	Phase	k^*
$q=n$	Any n	$n-1$	$\text{COS}(n-1)$	$2\pi p/n$
$q < n$	$n \neq 2$	—	COS0	$2\pi p/q$
$q > n$	Any n	n	$\text{CIS}(n-1)$	$2\pi p/q$

of a spatially inhomogeneous state with the corresponding wave number.

To analyze the stability of the homogeneous state, we generalize the procedure used by Marston and Affleck² to the one-third-filled case in the large- U limit. When n is an integer multiple of 3, the number of fermions sitting on each site is an integer in a homogeneous sample, and a finite energy is needed to add an extra particle. This energy gap at k_F may imply a tripling of the spatial period in the ground state. To search for this spatial inhomogeneity, a more general model, the SU(n) symmetric generalization of the Hubbard-Heisenberg model, will be considered. Its Hamiltonian is

$$H = \sum_{i=1}^N \left[-\frac{J}{n} \sum_{\sigma, \sigma'=1}^n (c_{i,\sigma}^\dagger c_{i+1,\sigma}) (c_{i+1,\sigma'}^\dagger c_{i,\sigma'}) - t \sum_{\sigma=1}^n (c_{i,\sigma}^\dagger c_{i+1,\sigma} + \text{H.c.}) + \frac{U}{n} \left(\sum_{\sigma=1}^n c_{i,\sigma}^\dagger c_{i,\sigma} - \frac{n}{3} \right)^2 \right]. \quad (20)$$

The rationale underlying this generalization is that the inclusion of an interaction between nearest neighbors allows us to study states with nonuniform bonds. Although we are interested in models with $n=3, 4, \dots$, the behavior of the model will be studied for large- n values since then the saddle-point method can be applied. The chemical potential is shifted to zero at one-third filling, and the Hubbard coupling U and Heisenberg coupling J are rescaled by $2/n$ so that the spacing of the energy levels remain the same as n increases. We note that the usual $J \sum_{\langle i,j \rangle} \mathbf{S}_i \cdot \mathbf{S}_j$ nearest-neighbor Heisenberg interaction breaks up into three terms in the fermionic representation of the spin operators. One of them only shifts the chemical potential, another corresponds to the nearest-neighbor Coulomb interaction (that is unimportant in the large U limit); therefore, they are neglected and only the third is kept.

The equilibrium state will be determined from the minimum of the free energy that can be derived from the partition function of the system. In functional integral formalism, the partition function can be expressed with the Lagrangian of the model. At finite temperatures, the imaginary time Lagrangian is $L[c, c^\dagger] = \sum_{i,\sigma} c_{i,\sigma}^\dagger (d/d\tau) c_{i,\sigma} + H$ and the partition function is

$$Z = \int [dc][dc^\dagger] \exp \left(- \int_0^\beta d\tau L[c, c^\dagger] \right). \quad (21)$$

Here, β is the inverse temperature. The integral occurring in the above expression cannot be calculated in a simple way due to the quartic terms in the Lagrangian. However, these quartic terms can be eliminated by a Hubbard-Stratonovich transformation based on the integral identity

$$\exp(VX^2) \propto \int dY \exp(-Y^2/4V + XY). \quad (22)$$

In our case, the quantities corresponding to X are $\sum_{\sigma} c_{i,\sigma}^\dagger c_{i,\sigma}$ and $\sum_{\sigma} c_{i,\sigma}^\dagger c_{i+1,\sigma}$. Therefore, we have to introduce $2N$ bosonic fields: ϕ_i and $\chi_{i,i+1}$. We note that the fields ϕ_i and $\chi_{i,i+1}$

correspond² to site- and bond-centered densities, respectively.

Adding the appropriate terms to the Lagrangian gives

$$L[c, c^\dagger, \phi, \chi] = L[c, c^\dagger] + \frac{n}{U} \sum_i \left[\frac{\phi_i}{2} + i \frac{U}{n} \left(\sum_\sigma c_{i,\sigma}^\dagger c_{i,\sigma} - \frac{n}{3} \right) \right]^2 + \frac{n}{J} \sum_i \left| \frac{1}{2} \chi_{i,i+1} + \frac{J}{n} \sum_\sigma c_{i,\sigma}^\dagger c_{i+1,\sigma} \right|^2. \quad (23)$$

The new Lagrangian is quadratic in the fields; however, the fermionic fields are coupled to the bosonic ones. The explicit form of the Lagrangian is

$$L[c, c^\dagger, \phi, \chi] = \sum_{i,\sigma} \left\{ c_{i,\sigma}^\dagger \left(\frac{d}{d\tau} + i\phi_i \right) c_{i,\sigma} + \frac{1}{4J} |\chi_{i,i+1}|^2 + [(\chi_{i,i+1} - t) c_{i,\sigma}^\dagger c_{i+1,\sigma} + \text{H.c.}] + \frac{1}{4U} \phi_i^2 - i \frac{1}{3} \phi_i \right\}. \quad (24)$$

The partition function is obtained by integrating over c and c^\dagger ,

$$Z[\phi, \chi] = \int [dc][dc^\dagger] \exp \left(- \int_0^\beta d\tau L[c, c^\dagger, \phi, \chi] \right). \quad (25)$$

Writing it in the form $Z[\phi, \chi] \equiv \exp(-S_{\text{eff}}[\phi, \chi])$, this defines the effective action. The free energy can be expressed in a usual way via $Z[\phi, \chi]$ as

$$F[\phi, \chi] = -1/\beta \ln Z[\phi, \chi]. \quad (26)$$

As mentioned in the previous subsection, if spatial oscillations occur in the system, they are expected to appear with wave number $k^* = 2\pi f$. Thus, we may expect a spontaneous trimerization at one-third filling. Therefore, we suppose that the boson field ϕ_i takes three different values depending on whether $i=3l$, $i=3l+1$, or $i=3l+2$ with integer l . They will be denoted as ϕ_1 , ϕ_2 , and ϕ_3 . Similar assumption holds for the fields $\chi_{i,i+1}$, too. The three values are χ_1 , χ_2 , and χ_3 . The lattice is thus decomposed into three sublattices.

To get a real free energy, the fields ϕ_α ($\alpha=1,2,3$) are redefined by continuing to the complex plane ($i\phi_\alpha \rightarrow \phi_\alpha$). The free energy can then be written as

$$F(\{\phi_\alpha\}, \{\chi_\alpha\}) = \frac{1}{3} \sum_{\alpha=1}^3 \left(\frac{Nn}{4J} \chi_\alpha^2 + \frac{Nn}{4U} \phi_\alpha^2 - \frac{Nn}{3} \phi_\alpha \right) + \frac{n}{3} \sum_k [E(k) - 1/3], \quad (27)$$

and the summation for k has to be performed over the reduced Brillouin zone which is now one-third of the original one (k runs from $-\pi/3$ to $\pi/3$) and $E(k)$ is the energy spectrum of a single fermion coupled to the boson fields. It is the eigenvalues of the Hamiltonian

$$H = \sum_i \{ [(\chi_1 - t) a_i^\dagger b_{i+1} + (\chi_2 - t) b_{i+1}^\dagger c_{i+2} + (\chi_3 - t) c_{i+2}^\dagger a_{i+3} + \text{H.c.}] + \phi_1 a_i^\dagger a_i + \phi_2 b_{i+1}^\dagger b_{i+1} + \phi_3 c_{i+2}^\dagger c_{i+2} \}, \quad (28)$$

where the operators a , b , and c belong to different sublattices. In order to determine the one-particle spectrum, one has to diagonalize the Hamiltonian [Eq. (28)] in momentum space. Therefore, we are looking for the eigenvalues of the matrix

$$\begin{pmatrix} \phi_1 & (\chi_1 - t)e^{-ik} & (\chi_3 - t)e^{ik} \\ (\chi_1 - t)e^{ik} & \phi_2 & (\chi_2 - t)e^{-ik} \\ (\chi_3 - t)e^{-ik} & (\chi_2 - t)e^{ik} & \phi_3 \end{pmatrix}. \quad (29)$$

The energy spectrum $E(k)$ has three branches corresponding to the three (real) solutions of the third-order eigenvalue equation

$$E_1(k) - (\phi_1 + \phi_2 + \phi_3)/3 = -\text{sgn}(Q) \sqrt{|P|} \cos \left[\frac{1}{3} \cos^{-1} \left(\left| \frac{Q}{(|P|)^{3/2}} \right| \right) \right], \quad (30a)$$

$$E_{2,3}(k) - (\phi_1 + \phi_2 + \phi_3)/3 = -\text{sgn}(Q) \sqrt{|P|} \cos \left[\frac{1}{3} \cos^{-1} \left(\left| \frac{Q}{(|P|)^{3/2}} \right| \pm \frac{2\pi}{3} \right) \right]. \quad (30b)$$

Here, P and Q are the parameters in the eigenvalue equation when transformed to the form $\tilde{E}^3(k) + P\tilde{E}(k) + Q = 0$ with $\tilde{E}(k) = E(k) - (\phi_1 + \phi_2 + \phi_3)/3$.

The minimum of the free energy of a system with such a spectrum cannot be evaluated quite generally. Fortunately, we are only interested whether the three ϕ_α and χ_α are different or not. This analysis can be carried out easier in terms of the linear combinations

$$\phi := (\phi_1 + \phi_2 + \phi_3)/3, \quad (31a)$$

$$\Delta\phi_1 := (\phi_1 - \phi_2)/2, \quad (31b)$$

$$\Delta\phi_2 := (\phi_1 + \phi_2 - 2\phi_3)/6, \quad (31c)$$

and similar definitions for χ , $\Delta\chi_1$, and $\Delta\chi_2$. One finds that although the free energy has an extremum at $\Delta\phi_1 = \Delta\phi_2 = 0$ and $\Delta\chi_1 = \Delta\chi_2 = 0$, the free energy of the uniform state is not a local minimum. Thus, a density wave has to appear in the system. We can conclude that the $SU(n)$ Hubbard model is unstable against the Heisenberg coupling in the large- n limit and exhibits inhomogeneous spatial ordering for $U > 0$.

From this analysis alone—due to the rather complicated one-particle spectrum—we cannot decide whether the system is dimerized, trimerized, or some other periodicity occurs, and whether the density wave is site centered or bond centered. It is natural to relate the nonuniform phase to the fully gapped excitation spectrum. Thus, when our previous considerations are taken into account, trimerized phase is expected in one-third-filled models. This will be supported by the numerical calculation. We will also see that the trim-

erized phase is not a special feature of the systems with integer number of electrons per site. It occurs in the one-third-filled system for arbitrary $n > 3$.

IV. NUMERICAL STUDY OF THE SPATIAL INHOMOGENEITY

In this section, we present our numerical results obtained by the DMRG³⁵ method for the length dependence of the block entropy $s_N(l)$ and its Fourier transform $\bar{s}(k)$ to relate them to the number and position of soft modes when the model is critical, or to spatial inhomogeneity of the ground state for gapped models.

The spatial modulation of the ground state can be a site- or a bond-centered density wave. A site-centered density wave would manifest itself in an oscillation of the von Neumann entropy of single sites, s_i , with $i=1, \dots, N$ or in the local electron density defined by

$$\langle n_i \rangle = \sum_{a=1}^n \langle \Psi_{\text{GS}} | n_{i,a} | \Psi_{\text{GS}} \rangle, \quad (32)$$

where $|\Psi_{\text{GS}}\rangle$ is the ground-state wave function. The wave number of the charge oscillation can again be determined from peaks in the Fourier transform of s_i or $\langle n_i \rangle$ denoted as $s_1(k)$ and $n(k)$, respectively.

The existence of a bond-centered density wave can be demonstrated by studying the variation of the bond energy or the two-site entropy along the chain. To avoid boundary effects, we have calculated the difference of two-site entropies in the middle of the chain, between first, second, third, and so on neighbor bonds,

$$D_s(N) = s_{N/2, N/2+1} - s_{N/2+1, N/2+2}, \quad (33a)$$

$$T_s(N) = s_{N/2, N/2+1} - s_{N/2+2, N/2+3}, \quad (33b)$$

$$Q_s(N) = s_{N/2, N/2+1} - s_{N/2+3, N/2+4}, \quad (33c)$$

$$P_s(N) = s_{N/2, N/2+1} - s_{N/2+4, N/2+5}. \quad (33d)$$

For convenience, the number of sites in the chain was always even. Moreover, since we expect dimerized, trimerized, or tetramerized phases depending on the commensurate filling p/q , the number of sites N was always taken to be an integer multiple of q .

When a doubling of the lattice periodicity of the ground state is indicated by a finite peak in $|\bar{s}(k)|$ at $k^* = \pi$, a truly dimerized phase gives equal finite values for D_s and Q_s and vanishing T_s and P_s in the $N \rightarrow \infty$ limit. Stronger and weaker bonds alternate along the chain. When the peak in $|\bar{s}(k)|$ appears at $k^* = 2\pi/3$ and a trimerized phase is expected, T_s should be finite and Q_s should vanish. Symmetry considerations imply that two equally strong bonds are followed by a weaker or stronger bond in this case. In a tetramerized phase, the peak in $|\bar{s}(k)|$ appears at $k^* = \pi/2$, D_s , T_s , and Q_s may be finite in the $N \rightarrow \infty$ limit and only P_s vanishes necessarily.

A. Numerical procedure

The numerical calculations presented in this paper have been performed on finite chains with open boundary condi-

tion (OBC) using the DMRG technique and the dynamic block-state selection approach.^{36,37} We have set the threshold value of the quantum information loss χ to 10^{-5} for $n=3, 4$ and to 10^{-4} for $n=5$ and the minimum number of block states M_{min} to 256. In spite of the large number of degrees of freedom per site in the $n=5$ case, the entropy analysis allows one to study this problem as well. The ground state has been targeted using four to eight DMRG sweeps until the entropy sum rule has been satisfied. The accuracy of the Davidson diagonalization routine has been set to 10^{-7} and the largest dimension of the superblock Hamiltonian was around 3×10^6 . As an indication of the computational resources used in the present work, we note that the maximum number of block states was around 1600 for $n=3$ and 900 for $n=4$ and 5.

The large- N limit of the entropies and amplitudes of the peaks in the Fourier spectrum can be obtained if appropriate scaling functions are used. In a critical, gapless model, in leading order, these are expected to scale to zero as $1/N$, while in a noncritical model, the scaling function depends on the boundary condition. Therefore, for any quantity A , the finite-size-scaling ansatz,

$$A(N) = A_0 + a/N^\beta, \quad (34)$$

is used to evaluate the data obtained with OBC, where A_0 , a , and β are free parameters to be determined by the fit.

B. Numerical results

1. Models with $q=n$

The $1/n$ -filled case ($q=n$) has already been considered in Ref. 9 and some of the results were listed in Sec. II. As has been shown in Fig. 1, $s_N(l)$ oscillates with period n for finite systems. These oscillations are due to the soft modes located at wave numbers $k^* = 2\pi/n$. Taking every n th value only, $s_N(l)$ can be fitted accurately using (3) for relatively short chains already if U is large. After a proper finite-size scaling, the fit gives $c=n-1$, as expected.

Taking the Fourier transform of $s_N(l)$, besides the large positive peak at $k=0$, additional negative peaks are found at the positions of the soft modes, at $k^* = \pi, 2\pi/3, \pi/4$, and $2\pi/5$ for $n=2, 3, 4, 5$, respectively. Their amplitude vanishes, however, in the $N \rightarrow \infty$ limit. As a further check that there are neither site- nor bond-centered oscillations in the ground state, we have analyzed s_i , $\langle n_i \rangle$, and $s_{i,i+1}$. All Fourier components of these quantities scale to zero in the thermodynamic limit. As an example, the finite-size dependence of $n(k^*)$ for $n=3$ and $n=4$ is shown in Fig. 6 at $U=10$.

When the finite-size scaling of D_s , T_s , and Q_s is analyzed, one finds that they all vanish in the thermodynamic limit, as shown in Figs. 7–9 for $U=10$. All this shows that the ground state of the $1/n$ -filled $SU(n)$ Hubbard model is spatially homogeneous; the translational symmetry is not broken.

2. Models with $q > n$

We have chosen as an example $n=3$ and $f=2/5$. As seen in Fig. 3(a), the block entropy $s_N(l)$ oscillates with period 5. When every fifth data points are fitted to (3), $c=3$ is ob-

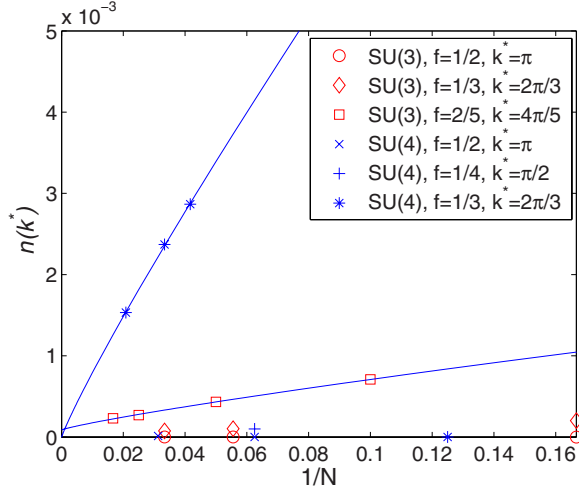


FIG. 6. (Color online) Finite-size dependence of $n(k^*)$ for various n and fillings for $U=10$. The solid line is the finite-size-scaling fit.

tained. This indicates that the model remains critical for finite U as well. The finite peak in $|\bar{s}(k)|$ at $k^*=4\pi/5$ is due to soft modes. The amplitude of the peak disappears in the $N \rightarrow \infty$ limit and the ground state of the system is uniform. This is confirmed by the calculation of $\bar{s}(k^*)$, $n(k^*)$, D_s , T_s , and Q_s shown in Figs. 2 and 6–9, respectively. There is neither a site- nor a bond-centered oscillation in the occupation number or bond strength.

3. Models with $q < n$

One realization of this condition, the half-filled case for $n > 2$, has been studied by us earlier.⁹ It was found, as shown in Fig. 1, that the block entropy oscillates with period 2 for any $n > 2$. The peak in $|\bar{s}(k)|$ at $k^*=\pi$ does not vanish in the thermodynamic limit (see Fig. 2). In agreement with this, D_s and Q_s are finite and converge to the same value, as shown in Figs. 7 and 9, while T_s vanishes (see Fig. 8). The same be-

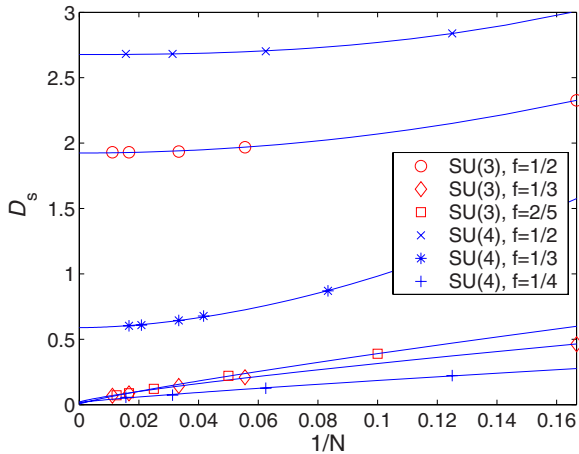


FIG. 7. (Color online) Finite-size dependence of D_s for various n and fillings for $U=10$. The solid line is the finite-size-scaling fit.

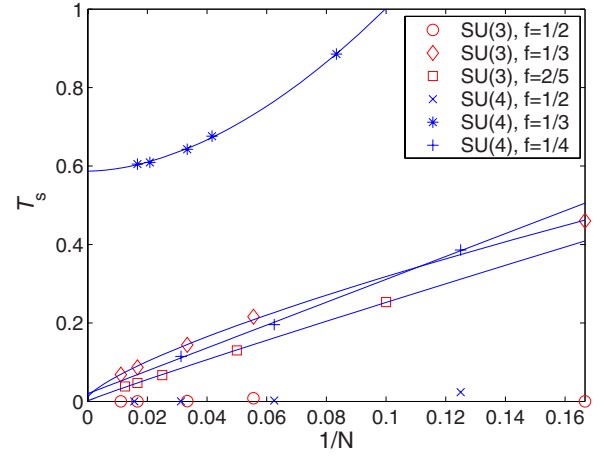


FIG. 8. (Color online) Finite-size dependence of T_s for various n and fillings for $U=10$. The solid line is the finite-size-scaling fit.

havior is found in the $n=5$ model at half filling, as seen in the upper panel of Fig. 10.

On the other hand, $s_1(k^*)$ and $n(k^*)$ vanish in the thermodynamic limit (see Fig. 6). The translational symmetry of the Hamiltonian is broken and the ground state of the half-filled model is dimerized. Stronger and weaker bonds alternate along the chain.

In the one-third-filled case of the $n=4$ and $n=5$ models ($q < n$), $s_N(l)$ oscillates with period 3 and the amplitude of the Fourier component $\bar{s}(k^*=2\pi/3)$ remains finite even for $N \rightarrow \infty$ (see Figs. 2 and 4). This indicates that the spatial periodicity is tripled in the ground state. This is corroborated by our results shown in Figs. 7–9 and the middle panel of Fig. 10. D_s and T_s scale to the same finite value while Q_s , $s_1(k^*)$ and $n(k^*)$ vanish. In the ground state, two bonds of equal strength are followed by a weaker or stronger bond.

As a last example, we have studied the quarter-filled SU(5) Hubbard chain. We found that $|\bar{s}(k)|$ scales to a finite value at $k^*=\pi/4$, as shown in Fig. 4. All Fourier components of the site entropy and local charge density vanish for long

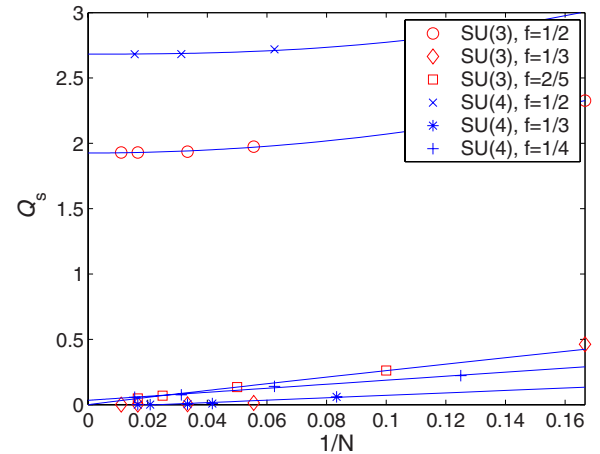


FIG. 9. (Color online) Finite-size dependence of Q_s for various n and fillings for $U=10$. The solid line is the finite-size-scaling fit.

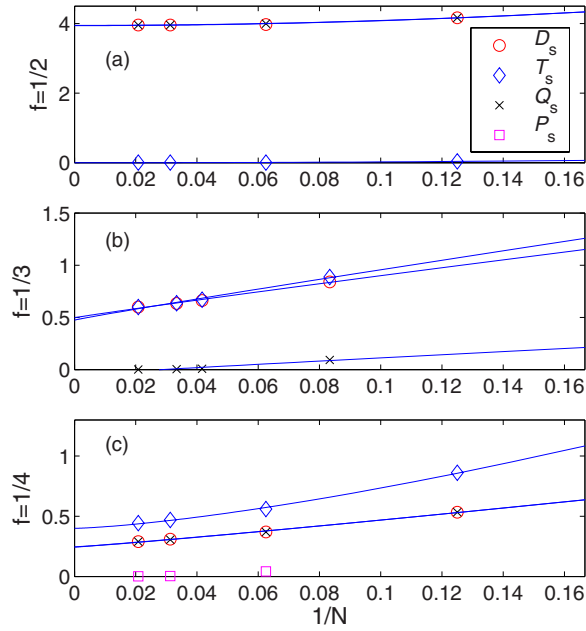


FIG. 10. (Color online) Finite-size dependence of D_s , T_s , Q_s , and P_s for the half-, one-third-, and quarter-filled one-dimensional SU(5) Hubbard models at $U=10$.

chains, while D_s , T_s , and Q_s scale to finite values. Only P_s scales to zero, as shown in the lower panel of Fig. 10. The ground state is a bond-ordered tetramerized state. Figure 11 shows schematically the periodic modulation of the bond strength along the chain for half-, one-third-, and quarter-filled models.

V. CONCLUSION

To study the role of multiparticle umklapp processes, we have treated the one-dimensional SU(n) Hubbard model analytically by bosonization approach and numerically using the DMRG method for $n=3, 4$, and 5 for commensurate fillings $f=p/q$, where p and q are relative primes.

Our results confirm that umklapp processes play essentially different roles depending on the relationship between q and n . When $q=n$ (this is the case in the $1/n$ -filled case),

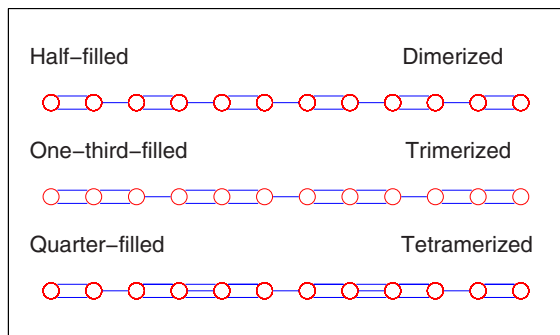


FIG. 11. (Color online) Schematic plot of the local bond strength in half-, one-third-, and quarter-filled SU(5) Hubbard chains.

TABLE II. Central charge and spatial inhomogeneity for the p/q -filled SU(n) Hubbard chain. k^* in the last column gives the wave number of soft modes when the model is critical, while it gives the wave number of the nonuniform ground state when the model is gapped.

	n	p/q	c	Periodicity	k^*
$q=n$	2	1/2	1	Uniform	π
	3	1/3	2	Uniform	$2\pi/3$
	4	1/4	3	Uniform	$\pi/2$
	5	1/5	4	Uniform	$2\pi/5$
$q<n$	3	1/2		Dimerized	π
	4	1/2		Dimerized	π
	4	1/3		Trimerized	$2\pi/3$
	5	1/2		Dimerized	π
	5	1/3		Trimerized	$2\pi/3$
$q>n$	5	1/4		Tetramerized	$\pi/2$
	3	2/5	3	Uniform	$4\pi/5$

the charge and spin modes are not coupled, and the umklapp processes open the gap only in the spectrum of charge modes. The system remains critical with $n-1$ gapless spin modes, the central charge is $c=n-1$, and the translational symmetry of the Hamiltonian is not broken in the ground state.

When $q>n$, the leading-order umklapp processes are forbidden in the model with local interaction by Pauli's exclusion principle. The model is equivalent to an n -component Luttinger liquid with $c=n$ and the ground state is spatially uniform for $U\geq 0$.

When, however, $q<n$, the charge and spin modes are coupled by the umklapp processes and the gap opens in the spectrum of all modes. Even more interestingly, a spatially nonuniform ground state emerges whose periodicity depends on the filling. Half-filled models develop a dimerized ground state, trimerized state appears in one-third-filled models, and the ground state is tetramerized in quarter-filled models. Other periodicities would probably be found at other fillings. Our findings are summarized in Table II, which can be compared to the analytical results given in Table I.

We emphasize that our calculations were performed at a relatively large value of U , where the nonuniformity of the ground state is well developed, and the finite value of the dimer, trimer, or tetramer order parameter can easily be detected. We conjecture, based on our earlier calculations,⁹ that the critical value U_c above which the nonuniform phase appears is $U_c=0$.

ACKNOWLEDGMENTS

This research was supported in part by the Hungarian Research Fund (OTKA) Grants Nos. K 68340, F 046356, and NF 61726 and the János Bolyai Research Fund. The authors acknowledge computational support from Dynaflex Ltd. under Grant No. IgB-32.

- ¹J. Hubbard, Proc. R. Soc. London, Ser. A **276**, 238 (1963); **277**, 237 (1964); **281**, 401 (1964); **285**, 542 (1965).
- ²J. B. Marston and I. Affleck, Phys. Rev. B **39**, 11538 (1989).
- ³R. Assaraf, P. Azaria, M. Caffarel, and P. Lecheminant, Phys. Rev. B **60**, 2299 (1999).
- ⁴R. Assaraf, P. Azaria, E. Boulat, M. Caffarel, and P. Lecheminant, Phys. Rev. Lett. **93**, 016407 (2004).
- ⁵C. Honerkamp and W. Hofstetter, Phys. Rev. Lett. **92**, 170403 (2004).
- ⁶F. F. Assaad, Phys. Rev. B **71**, 075103 (2005).
- ⁷E. Szirmai and J. Sólyom, Phys. Rev. B **71**, 205108 (2005).
- ⁸E. Szirmai and J. Sólyom, Phys. Rev. B **74**, 155110 (2006).
- ⁹K. Buchta, Ö. Legeza, E. Szirmai, and J. Sólyom, Phys. Rev. B **75**, 155108 (2007).
- ¹⁰Á. Rapp, G. Zaránd, C. Honerkamp, and W. Hofstetter, Phys. Rev. Lett. **98**, 160405 (2007).
- ¹¹J. Zhao, K. Ueda, and X. Wang, arXiv:cond-mat/0702582 (unpublished).
- ¹²T. J. Osborne and M. A. Nielsen, Phys. Rev. A **66**, 032110 (2002).
- ¹³A. Osterloh, L. Amico, G. Falci, and R. Fazio, Nature (London) **416**, 608 (2002).
- ¹⁴P. Zanardi, Phys. Rev. A **65**, 042101 (2002).
- ¹⁵S.-J. Gu, H.-Q. Lin, and Y.-Q. Li, Phys. Rev. A **68**, 042330 (2003).
- ¹⁶J. Vidal, G. Palacios, and R. Mosseri, Phys. Rev. A **69**, 022107 (2004); J. Vidal, R. Mosseri, and J. Dukelsky, *ibid.* **69**, 054101 (2004).
- ¹⁷M.-F. Yang, Phys. Rev. A **71**, 030302(R) (2005).
- ¹⁸S.-J. Gu, S.-S. Deng, Y.-Q. Li, and H.-Q. Lin, Phys. Rev. Lett. **93**, 086402 (2004).
- ¹⁹L.-A. Wu, M. S. Sarandy, and D. A. Lidar, Phys. Rev. Lett. **93**, 250404 (2004).
- ²⁰Ö. Legeza and J. Sólyom, Phys. Rev. Lett. **96**, 116401 (2006).
- ²¹W. K. Wootters, Phys. Rev. Lett. **80**, 2245 (1998).
- ²²P. Zanardi and N. Paunković, Phys. Rev. E **74**, 031123 (2006); P. Zanardi, M. Cozzini, and P. Giorda, arXiv:quant-ph/0606130 (unpublished).
- ²³G. Vidal, J. I. Latorre, E. Rico, and A. Kitaev, Phys. Rev. Lett. **90**, 227902 (2003).
- ²⁴Ö. Legeza, J. Sólyom, L. Tincani, and R. M. Noack, Phys. Rev. Lett. **99**, 087203 (2007).
- ²⁵V. E. Korepin, Phys. Rev. Lett. **92**, 096402 (2004).
- ²⁶C. Holzhey, F. Larsen, and F. Wilczek, Nucl. Phys. B **424**, 443 (1994).
- ²⁷P. Calabrese and J. Cardy, J. Stat. Mech.: Theory Exp. (2004) P06002.
- ²⁸I. Affleck and A. W. W. Ludwig, Phys. Rev. Lett. **67**, 161 (1991).
- ²⁹N. Laflorencie, E. S. Sørensen, M.-S. Chang, and I. Affleck, Phys. Rev. Lett. **96**, 100603 (2006).
- ³⁰J. Zinn-Justin, *Quantum Field Theory and Critical Phenomena* (Clarendon, Oxford, 2001).
- ³¹J. Sólyom, Adv. Phys. **28**, 201 (1979).
- ³²For a review, see A. O. Gogolin, A. A. Nersisyan, and A. M. Tsvelik, *Bosonization and Strongly Correlated Systems* (Cambridge University Press, Cambridge, 1998).
- ³³F. D. M. Haldane, J. Phys. C **14**, 2585 (1981).
- ³⁴T. Giamarchi and A. J. Millis, Phys. Rev. B **46**, 9325 (1992).
- ³⁵S. R. White, Phys. Rev. Lett. **69**, 2863 (1992); Phys. Rev. B **48**, 10345 (1993).
- ³⁶Ö. Legeza, J. Röder, and B. A. Hess, Phys. Rev. B **67**, 125114 (2003).
- ³⁷Ö. Legeza and J. Sólyom, Phys. Rev. B **70**, 205118 (2004).